Structural and electronic properties of K_nC_{60}

José Luís Martins
Department of Chemical Engineering and Materials Science, University of Minnesota, Minneapolis, Minnesota 55455

N. Troullier
Department of Chemical Engineering and Materials Science, University of Minnesota, Minneapolis, Minnesota 55455 and NEC Research Institute, Inc., Princeton, New Jersey 08540

(Received 3 December 1991)

We present local-density pseudopotential calculations of the structural and electronic properties of potassium fulleride K_nC_{60} ($n = 1, 2, 3, 6$) crystals, with an emphasis on the superconducting K_3C_{60} phase. The calculated enthalpies of reaction for all of the potassium fullerides are within 1.4–1.7 eV per K atom. The pressure-versus-volume equation of state indicates that K_3C_{60} is less compressible than C_{60}. The band structure of K_3C_{60} is very similar to that of C_{60}, and we discuss how it changes with pressure. Using calculated valence charge densities, we show that the valence electrons of the K atoms are almost completely transferred to the lowest unoccupied bands of the C_{60} molecular solid.

I. INTRODUCTION

Fullerene, C_{60}, is a spheroidal "soccer-ball" shaped molecule[1] with icosahedral symmetry, where all of the 60 carbon atoms occupy equivalent sites. The recent production of this molecule in macroscopic quantities[2] has generated a large interest in its solid-state properties. Solid C_{60} is a semiconductor, but upon exposure to alkali-metal vapors, films with moderate electrical conductivity can be obtained.[3] Superconductivity has been observed for the compound K_3C_{60} with an onset temperature[4] of $T_c = 18$ K. Superconductivity has subsequently been observed for other A_3C_{60} phases, with A an alkali metal, and with values of T_c that scale with the compound lattice constant, reaching $T_c = 31.3$ K for Rb_2CsC_{60}.[5] These remarkably high values are two orders of magnitude larger than those observed in graphite intercalated with alkali atoms,[6] raising fundamental questions about the mechanisms for superconductivity in the alkali-metal–fullerides. Here we present detailed local-density calculations of the structural and electronic properties of K_3C_{60}.

Solid C_{60} (fullerite) crystallizes in the fcc structure with a lattice constant of 14.2 Å, corresponding to a 10-Å separation between molecular centers.[2,7–10] Each C_{60} molecule has two types of bonds with lengths[11,12] 1.40 and 1.45 Å, respectively, which are characteristic of aromatic C-C bonds. The diameter of the molecule is $\sim$ 7.05 Å. The closest C-C distance between carbon atoms from neighboring C_{60} molecular units is $\sim$ 3.2 Å. This is slightly smaller than the 3.45-Å distance found between graphite planes, but it still indicates that the interaction between the C_{60} molecules is weak.

The alkali metals, and a few other elements such as the alkaline earths, form interstitial alloys with C_{60}. Present evidence indicates that at saturation all the alkali metals form a semiconducting phase with A_6C_{60} stoichiometry. K_6C_{60} and Cs_6C_{60} have a body-centered-cubic structure where the alkali atoms occupy all the quasitetrahedral interstitial sites between the large C_{60} molecules.[13] A body-centered-tetragonal[14,15] semiconducting phase of K_4C_{60} and Rb_4C_{60} has also been identified. Metallic phases occur for K_3C_{60}, Rb_3C_{60}, and for a few $A_{3-x}B_xC_{60}$ mixed phases with A, B=K, Rb, and Cs. K_3C_{60} has a face-centered-cubic lattice with the potassium atoms occupying both the two interstitial tetrahedral sites and the octahedral interstitial sites.[16] There is experimental evidence[17] for Li and Na fulleride semiconducting phases with stoichiometries Li_2C_{60} and Na_2C_{60} but their structure has not yet been determined. The phase diagram of the alkali-metal–fullerides turns out to be quite rich, with both semiconducting and metallic phases.

We present a study of the structural and electronic properties of the K_nC_{60} crystals, with a strong emphasis on the K_3C_{60} phase. A similar study of the C_{60} molecular crystal was the object of a recent paper[18] and we will frequently refer the reader to that work. In the next section we will briefly review the computational method. In Sec. III we present the structural properties, in Sec. IV we show the band structure, and in Sec. V we discuss charge transfer from K to C_{60}. The results are summarized in Sec. VI.

II. COMPUTATIONAL METHOD

The electronic structure of the K_nC_{60} ($n = 1, 2, 3, 6$) crystals was calculated using the first-principles pseudopotential local-density method.[19] C_{60} forms a solid with cubic close packing of the quasispherical molecules. Here we assume that the lattice is face centered cubic and that the crystal structure is tetrahedral with the space group T_h^3 ($Fm3$). The properties of KC_{60}, K_2C_{60}, and K_3C_{60} are calculated for the structures obtained by filling, respectively, the fcc octahedral interstices, the two

tetrahedral interstices, and both the octahedral and the two tetrahedral interstices of fcc C_{60}. In the T_h^3 configuration the C_{60} molecules are oriented with hexagonal faces in the (111) direction, thereby increasing the available space for alloying atoms in the smaller tetrahedral interstitial sites. This is the structure experimentally observed for K_3C_{60} neglecting the orientational superstructure of the C_{60} molecules.[16] There are two ways of putting a C_{60} molecule in a fcc lattice with the hexagons facing the tetrahedral interstices, and the x-ray spectra[16] are consistent with structural disorder associated with these two possible molecular orientations. The KC_{60} and K_2C_{60} crystals have not been experimentally observed; we use them as hypothetical structures in order to study the effects of occupying only one type of the available fcc interstitials. For K_6C_{60} we assume a bcc geometry[13] with the K atoms located at the $\frac{1}{4}, \frac{1}{2}, 0$ quasitetrahedral interstitial positions. In the real structure the potassium atoms are slightly displaced from these positions so that they are above the pentagonal and hexagonal faces. This displacement is associated with the tetrahedral symmetry of the molecule. In our calculations the bond lengths within the C_{60} molecule were kept fixed at the calculated equilibrium values[18,20] for pure C_{60}, 1.382 and 1.444 Å for the hexagon shared bond and for the pentagon edge, respectively. We monitored the forces on the carbon atoms in order to estimate corrections to the energy and geometry of the C_{60} molecular unit, and found that they were usually small.

The wave functions were expanded in a large basis set containing all plane waves with energies less than a chosen cutoff energy, $E_{\rm cut}$ = 49 Ry, and we used a "soft" pseudopotential.[21] With this combination of cutoff energy and pseudopotential, the total energy of all the systems studied was converged to within 0.05 eV/atom. This small energy correction for basis-set size was systematically included in all reported values of the calculated energies. The basis set contained ~19 000 to ~31 000 plane waves, depending on the unit-cell volume, and highly efficient iterative methods were used to diagonalize the Hamiltonian.[22,23] Because of the small size of the Brillouin zone of K_nC_{60}, two special **k** points are sufficient to calculate accurately the self-consistent screening potential. Using only the Γ point for Brillouin-zone integrals has a small but noticeable effect in the accuracy of the calculations. For example, the enthalpies of formation of K_nC_{60} would have been underestimated by ~0.3 eV per K atom if we had used the single Γ point, instead of the two special points.

The carbon pseudopotential was generated in the ground-state valence configuration $2s^22p^2$. The radial cutoffs, i.e., the radius at which inside this point the pseudo-wave-functions are allowed to deviate from the all-electron wave functions, were $r_{cs}=r_{cp}=1.50a_0$. We used the p potential as the local component and neglected the nonlocality of the d and higher scattering channels. The potassium pseudopotential was generated in the $4s^14p^0$ valence ground state using radial cutoffs of $r_{cs}=3.66a_0$ and $r_{cp}=3.80a_0$. We also included in the generation of the potassium pseudopotential an exchange-correlation pseudocore correction.[24] This was required because the $3p$ core orbitals of the potassium atoms are quite extended, and have a significant overlap with the $4s$ valence states. In test cases with bcc metallic potassium, the calculated lattice constant and cohesive energy without the core correction were 2.4% and 2.2% smaller, respectively, than the experimental values. Using a pseudopotential generated with the core correction improved the lattice constant to 0.9% smaller and the cohesive energy to 1.9% larger than the experimental data. For potassium, we use the s potential as the local component, and we neglect the nonlocal contributions to the d and higher scattering channels. The nonlocal p component of the potassium and the nonlocal s component of the carbon pseudopotential were transformed into separable operators.[25] We verified the absence of ghost states by checking the logarithmic derivatives of the separated pseudopotentials and by using the theorem of Gonze, Käckell, and Scheffler.[26]

III. STRUCTURAL PROPERTIES

In Table I, we give the calculated enthalpy of reaction for K_nC_{60} ($n = 1,2,3,6$) crystals and the number of alkali atoms surrounding each C_{60} molecule. The reference energies for the enthalpies of reaction are the total energies calculated for the C_{60} crystal in the fcc-T_h^3 symmetry and the bcc potassium metal, using the same pseudopotentials and energy cutoffs for the plane-wave expansion. We have neglected distortions of the individual C_{60} molecules due to the presence of the potassium atoms. This introduces a correction to the energies of Table I that we can estimate from the calculated atomic forces and from the force constants that we have previously determined in the optimization of the C_{60} molecular geometry.[18] Our estimates agree with a recent molecular-dynamics simulation[27] of K_6C_{60}, where it was found that optimizing the internal coordinates lowered the energy by ~1 eV, or ~0.2 eV per potassium atom. The energy gained by the relaxation of the internal coordinates of K_3C_{60} was smaller, and for the two other systems, K_2C_{60} and KC_{60}, it is even smaller. Therefore, the correction in Table I due to relaxation of the C_{60} molecules is at most ~0.2 eV per potassium atom.

TABLE I. The calculated enthalpies of reaction, ΔH^0_{rxn}, for K_nC_{60} ($n = 1,2,3,6$) structures. Also listed is the coordination number N_C for the number of potassium atoms surrounding each C_{60} molecular unit. All energies are in eV per potassium atom. The enthalpies are referenced to the calculated total energy for the bcc potassium metal and the fcc C_{60} solid. The lattice for the compounds are indicated in parentheses and their structure is given in the text. The negative values of ΔH^0_{rxn} indicate that the compounds are stable.

	ΔH^0_{rxn} (eV)	N_C
KC_{60} (fcc)	−1.4	6
K_2C_{60} (fcc)	−1.4	8
K_3C_{60} (fcc)	−1.7	~14
K_6C_{60} (bcc)	−1.7	24

The C_{60} potassium alloys have a moderate enthalpy of reaction of 1.4 to 1.7 eV per K atom (Table I). There is some correlation between the coordination number of the doping sites and the calculated enthalpy of reaction. If we assume a packing of hard C_{60} spheres, then the sizes of the fcc-octahedral, fcc-tetrahedral, and bcc-tetrahedral holes for the fcc C_{60} lattice are, respectively, ~4.3, ~2.3, and ~2.9 Å in diameter. According to Pauling's rules,[28] all of these sites can accommodate a K^+ ion of radius[29] 1.33 Å, if we take into account the extra room at the tetrahedral interstitials associated with the "dimples" at the center of the hexagons and pentagonal faces when we replace the hard "C_{60} sphere" by a model consisting of atomic spheres with the carbon van der Waals radius. The Madelung energy for $K^+C_{60}^-$ is 2.5 eV, so the calculated enthalpies of reaction are consistent with the values expected for ionic bonding between K cations and C_{60} anions. Our enthalpies of reaction disagree with a recent local-density calculation which found a value of ~10 eV per K atom.[30]

Our numerical results predict that K_6C_{60} is 0.04 eV per K atom more stable than K_3C_{60}, that is, the last phase is not stable, in disagreement with the experimental observation of a stable K_3C_{60}. However, the calculated energy difference is smaller than the numerical and physical accuracies of the present calculation, which are of the order of a tenth of an eV. What we can conclude from Table I is that the energy difference between alkali-metal–fullerides with different stoichiometries is small, and therefore the stoichiometry of the stable phases that will appear in the C_{60}-A_6C_{60} phase diagrams is a matter of a delicate energy balance, in the scale of a few hundredths of an eV. The fact that Li_3C_{60}, Na_3C_{60}, and Cs_3C_{60} have not yet been identified experimentally suggests that indeed the C_{60}-A_6C_{60} phase diagram depends on subtle differences between the alkali atoms. At the moment, the best explanation for the absence of those phases may still be that the Cs atoms are too large for the fcc-tetrahedral interstitials while the Li and Na atoms are too small for the fcc-octahedral interstitials.

In Table II we give the values for the equilibrium lattice constant, the bulk modulus, and the pressure derivative of the bulk modulus of K_3C_{60}. They were calculated by fitting total energies calculated at seven lattice constants in the range of 12.9–14.9 Å to the equations of state of Murnaghan,[31] Birch-Murnaghan,[32] and Vinet *et al.*[33] The small scatter in the parameters from the different equations of state illustrates the consistency of the fits. In Fig. 1 we show the equation of state, volume versus pressure, for K_3C_{60} and compare it to our previous calculation for C_{60}.[18] Both curves are from the fit to the Vinet *et al.*[33] equation of state. In Fig. 1 we can see that K_3C_{60} is only slightly stiffer than C_{60}. As will be discussed below, K donates its valence electron to C_{60} and therefore in both cases it is the rather weak intermolecular bonds that are being compressed. The calculated lattice constant of K_3C_{60} is ~14.19 Å, which is ~0.16 Å larger than the calculated C_{60} lattice constant

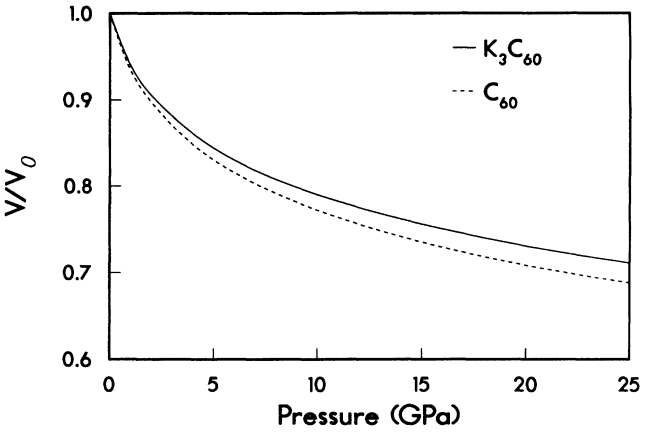

FIG. 1. The volume vs pressure equation of state for solid K_3C_{60} (solid line) and C_{60} (Ref. 18) (dashed line). The lines are obtained from fitting the calculated total energy at several lattice constants to the Vinet *et al.* (Ref. 33) equation of state. From the two curves we can see that K_3C_{60} is harder than C_{60}.

TABLE II. The calculated equilibrium lattice constant a, bulk modulus B_0, pressure derivative of the bulk modulus B_0', and enthalpy of reaction, ΔH_{rxn}^0, for K_3C_{60} are compared to experiment. The values are from fits of the calculated total energy to the equations of states of Murnaghan (Ref. 31), Birch-Murnaghan (Ref. 32), and Vinet *et al.* (Ref. 33). The enthalpy of reaction is per potassium atom, and is referenced to the calculated total energy for fcc C60 and bcc metallic potassium. The negative values of ΔH_{rxn}^0 indicate that K_3C_{60} is stable with respect to metallic potassium and C_{60} carbon.

	Ref. 31	Ref. 32	Ref. 33	Experiment
a (Å)	14.21	14.17	14.20	14.253,[a] 14.24[b]
B_0 (GPa)	24	23	22	28.0[c]
B_0'	9	14	11	
ΔH_{rxn}^0 (eV/K atom)	−1.64	−1.69	−1.66	

[a]Reference 5.
[b]Reference 16.
[c]Reference 34.

and is in good agreement with the experimental value of 14.253 Å.[5] The predicted bulk modulus is ~23.3 GPa, which is larger than the value of ~17.4 GPa calculated for C_{60}, and is 16% smaller than the experimental value of 28 GPa.[34]

IV. BAND STRUCTURE

The electronic structure of solid C_{60} has been described in our previous work,[18,20,35,36] which includes a paper with detailed local-density calculations for the structural and electronic properties of C_{60}.[18] The agreement between the density of states of C_{60} calculated with the first-principles local-density approximation and the features of the experimental electron photoemission[35] and inverse-photoemission[36] spectra was excellent. Because of the weakness of the intermolecular interactions and the high symmetry (I_h) of molecular C_{60}, the electronic structure of solid C_{60} (fullerite) consists of several "minibands" associated with the molecular states. These molecular states can be characterized as being of σ or π character, and have wave functions with a dominant angular momentum component with respect to the center of the molecule.[18,20,37] The molecular character of the solid is responsible for the sharp features observed in both the photoemission and inverse-photoemission spectra.

In Fig. 2 we show the band structure for K_3C_{60} plotted along the Δ, Λ, and Z directions of the fcc Brillouin zone calculated for a lattice constant of 14.24 Å. Figure 2 shows only bands 116 to 126, which are those close to the Fermi level. The wave functions associated with the lowest set of five bands of the figure have one radial nodal surface and have angular character $l = 5$ with respect to the center of the molecule, hence the label π_5. This set of bands is derived from the h_u fivefold-degenerate highest occupied molecular orbital (HOMO) of C_{60}. The middle set of bands is also of the π_5 type and are derived from the t_{1u}, threefold-degenerate, lowest unoccupied molecular orbital (LUMO) of C_{60}. The top set of bands has $l = 6$ angular character, is the lowest of the π_6 states, and is derived from a t_{1g} molecular state. The Fermi level in Fig. 2 is at 1.34 eV and is shown by the dashed line. Comparing the K_3C_{60} band structure to the C_{60} band structure[18] at the same lattice constant shows only small differences, on the order of a few meV. This shows that the π system of C_{60} shifts rigidly upon alloying with potassium. Our calculated band structure for K_3C_{60} is in good agreement with two local-density band-structure calculations using Gaussian orbitals.[38,39] It does not agree with a recent pseudopotential calculation with a small Gaussian basis set.[30]

In Fig. 3, we plot the band structure of K_3C_{60} at a lattice constant of 13.62 Å corresponding to a pressure of ~3 GPa. The same set of eleven individual bands (three groups of bands) of Fig. 2 is shown. Bands from below the π_5 HOMO-derived band are responsible for the avoided crossings near the X point. On the top of the figure, another π_5 band just crosses the top π_6 band near the Z direction. These bands were deleted from the figure for ease of comparison. The π_5 HOMO-derived band widened by 0.38 eV, the π_5-LUMO derived band is 0.22 eV wider, and the π_6 band is 0.30 eV wider. At the same time the gap between HOMO-derived and LUMO-derived bands narrowed by 0.35 eV. With increasing pressure, the π_5 LUMO-derived bands become lower in energy at the Γ point than at the X point, and at ~15 GPa the Γ point of the π_5 LUMO-derived bands becomes lower than the X point of the π_5 HOMO-derived bands.

The width of the half-filled π_5-t_{1u} group of bands of K_3C_{60} is $W = 0.41$ eV, and the dependence of the bandwidth on volume is given by $dW/d\ln V = -2.09$ eV.

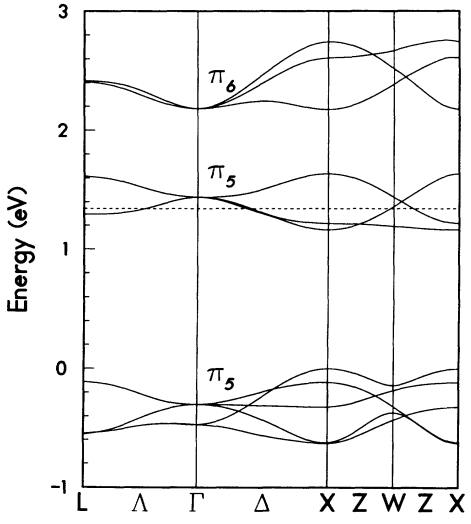

FIG. 2. The band structure of K_3C_{60} is plotted near the Fermi level at a pressure of ~ 0 GPa. The Fermi level is indicated by the dashed line. Comparing this plot to a similar C_{60} band structure (Ref. 18), we find that the inclusion of the potassium atoms into the C_{60} crystal introduce only minor alterations in the band structure in this energy range.

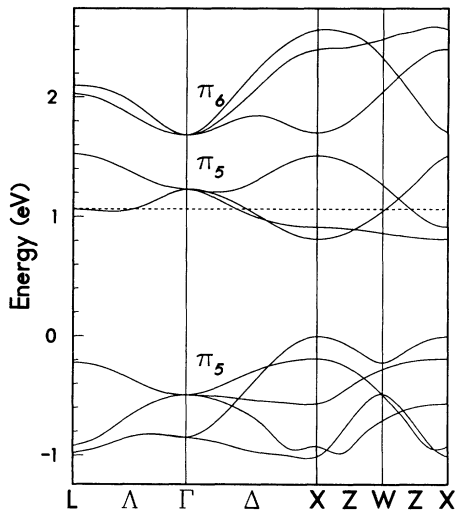

FIG. 3. The band structure of K_3C_{60} is plotted near the Fermi level at a pressure of ~3 GPa. The Fermi level is indicated by the dashed line. Comparing this to the zero-pressure band structure (Fig. 2), we see that band dispersion has noticeably increased.

Assuming that a typical value of the density of states at the Fermi level is given by $N(E_F) \approx 3/W$ we obtain the density of states of $N(E_F) \approx 7.2$ states per eV per spin and per C_{60}, and a derivative with respect to volume of $dN(E_F)/d \ln V \approx 36$ states per eV per spin and per C_{60}. Using the calculated compressibility, the pressure dependence of the density of states is $dN(E_F)/dp \approx -1.6$ eV^{-1} GPa^{-1} per spin and per C_{60}. The question of the experimental value of $N(E_F)$ for K_3C_{60} is still under debate.[40] One photoemission result suggests a value of 1–2 states per eV per spin and per C_{60},[41] while a value of $\sim$ 20 states per eV per spin and per C_{60} was obtained from NMR.[42] The density of states extracted from experiment includes renormalization factors due to electron-electron and electron-phonon interactions. These renormalization factors are different for different experimental situations. Since we do not know the magnitude of the renormalization factors we cannot yet make a direct comparison of the calculated density of states to the values extracted from experiment. Erwin and Pickett[38] calculated a density of states at the Fermi level of $N(E_F) = 6.6$ states per eV per spin and per C_{60} for a conduction band of K_3C_{60} with a width of $W = 0.6$ eV. Although local density underestimates band gaps it gives reasonable values for their pressure dependence. We found for K_3C_{60} that the volume dependence of the gap between HOMO- and LUMO-derived states is given by $dE_g/d \ln V = 2.6$ eV. Using a calculated bulk modulus of 23 GPa we obtain $dE_g/dp = -0.11$ eV/GPa. Using the experimental estimation of $\sim$1.6 eV for the excitation gap,[43] we find that it should close for a pressure of $\sim$15 GPa.

In Table III we compare the energies of conduction-band states of C_{60} to the corresponding states in K_3C_{60} at 0 GPa and $\sim$3 GPa. In column one we give the wave-function label[18] and its degeneracy. In columns two through four we give the eigenvalues at the Γ point for C_{60} and K_3C_{60} at zero pressure and at a pressure of $\sim$3 GPa. All the energies are in eV, and are referenced to the Γ-point energy of the equivalent π_5 HOMO-derived band. The π and σ molecular states of C_{60} and zero-pressure K_3C_{60} have similar eigenvalues (Table III). The nonmolecular states show appreciable deviations between fullerite and the alkali-metal–fulleride alloys. The C_l and O_l states, which are centered in the middle of the C_{60} molecule and on the octahedral holes, have a considerable decrease in energy relative to the surrounding states. These states are the fullerene equivalent of the interlayer states of graphite. Both the octahedral interstitial and the center of the C_{60} correspond to regions of very low electron density. The added three potassium valence electrons are transferred to the C_{60} molecule, increasing the electron-electron repulsion for the molecular states, and therefore increasing their energy relative to the C_l and O_l states. This effect is smaller for the tetrahedral states, T_{Al} and T_{Bl}, because the tetrahedral interstitial sites are smaller in size, and there is a smaller spatial separation between the tetrahedral electron states and the π and σ molecular orbitals. As the pressure on K_3C_{60} is increased to $\sim$3 GPa, the C_l and O_l states, residing in the large endohedral and octahedral holes, seem insensitive to pressure. However, states localized on the small tetrahedral interstitials and are forced upward in energy with increasing pressure. At higher pressures we find that the O_l states start shifting upwards in energy due to the reduction of the octahedral interstitial volume.

TABLE III. Comparison of the energies of the empty electronic states at the point Γ between C_{60}, K_3C_{60} at $\sim$0 GPa, and K_3C_{60} at $\sim$3 GPa. The wave functions are labeled according to their symmetry in the tetrahedral space group and their type (e.g., σ, π, C, O, and T orbitals, see text) and by the dominant angular momentum l with respect to the molecular center. All energies are in eV, and are referenced to the highest occupied state at Γ.

Label	C_{60}	K_3C_{60} (0 GPa)	K_3C_{60} ($\sim$3 GPa)
π_5-t_u	0.000	0.000	0.000
π_5-t_u	1.710	1.740	1.724
π_6-t_g	2.372	2.482	2.178
π_5-t_u	3.469	3.459	3.345
π_6-e_g	4.052	3.937	4.007
π_6-t_g	4.103	3.987	4.104
C_0-a_g	4.217	3.533	4.083
π_7-e_u	4.971	5.016	4.802
π_6-a_g	5.149	5.005	4.889
π_7-t_u	5.515	5.328	5.371
σ_9-a_u	5.878	5.737	5.557
π_6-t_g	6.240	6.062	6.312
σ_9-t_u	6.423	6.248	6.321
O_0-a_g	6.495	6.055	6.185
T_{0A}-a_u	6.974	6.595	8.025
T_{0B}-a_g	7.212	7.187	8.131
C_1-t_u	7.430	6.466	7.160
σ_{10}-t_g	7.454	7.179	7.498
σ_9-t_u	7.815	7.377	7.800

V. CHARGE TRANSFER

We found that when C_{60} is alloyed with K, a very electropositive element, the valence electron from the K atom is almost completely transferred to the lowest unoccupied bands of the C_{60} molecule. Figure 4(a) shows a contour plot of the total valence (pseudo)charge density of C_{60} in a (110) plane. In that panel the intersection of the plane with two halves of C_{60} molecules centered on the left and right edges of the figure can be clearly seen. The small overlap of the charge densities between the two molecules is another sign of the molecular character of solid C_{60}. In Fig. 4(b) we show in the same (110) plane a contour plot of the sum of the square of the wave functions for the three LUMO-derived π_5-t_u at the Γ point. Near the center of Fig. 4(b) we see two characteristic carbon π bonds, one on each of the two molecules, and which show a small intermolecular overlap. These two bonds correspond to a pentagon edge on each of the molecules that are very close to the (110) plane. At the edge of the figure the (110) plane intersects a hexagon-hexagon bond. All the hexagon-hexagon bonds are crossed by a nodal surface of the t_{1u} orbitals[18] and therefore there is a very small weight of the square of the wave functions on those regions. In Fig. 4(c) we show a contour plot obtained by subtracting the total valence charge density of C_{60} from the total charge density of

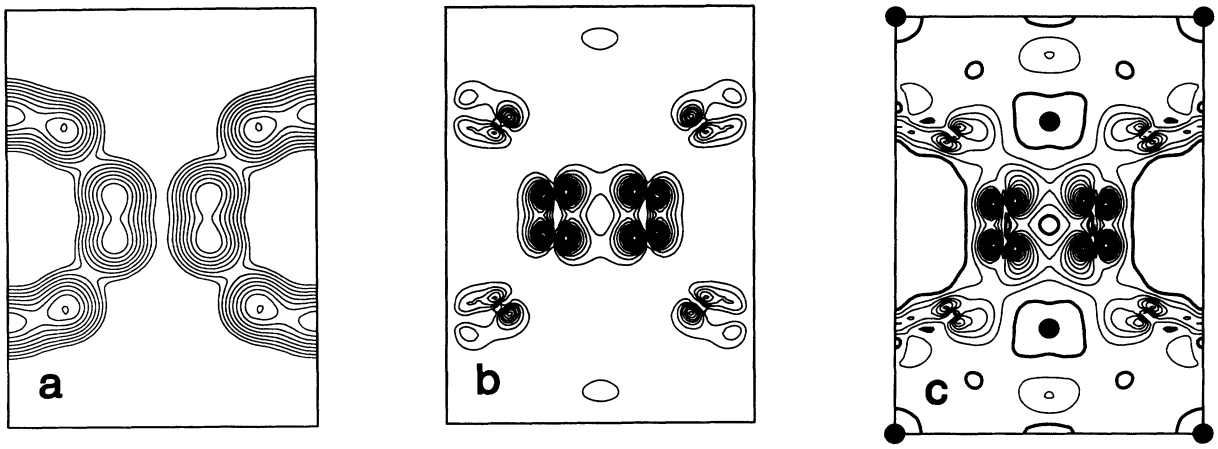

FIG. 4. Contour plots of the (pseudo)valence charge density for two adjacent molecules in the (110) plane of fcc C_{60} and K_3C_{60}. (a) The total valence charge density of C_{60} with a logarithmic spacing of the contours from 68.1 to 1000 electrons/cell. The charge density is concentrated near the surface of the C_{60} spheres. (b) The sum of the squares of the three lowest unoccupied π_5 orbitals at the Γ point (t_{1u} molecular symmetry). The overlap between the neighboring orbitals is clearly visible at the center of figure. The wave functions are larger outside than inside the C_{60} spheres as a consequence of *sp* hybridization. (c) The difference in total charge densities between K_3C_{60} and C_{60}. By comparison with panel (b) we conclude that the three extra electrons of K_3C_{60} are associated with the empty LUMO-derived orbitals of C_{60}. The location of the K atoms in (c) is indicated by the filled circles, and the heavy solid lines separate the regions of charge depletion (note that there exist no regions of high charge depletion) from the regions of charge increase. In both (b) and (c) the contours are spaced linearly by 2.5 electrons/cell.

K_3C_{60}. This shows the regions in the crystal where the three added electrons can be found. The similarity of Figs. 4(b) and 4(c) indicates that the K valence electrons are transferred to the LUMO-derived states of C_{60}. We observed a similar charge transfer to the LUMO-derived states for the other K fullerides, K_nC_{60} ($n = 1, 2, 3, 6$).

VI. SUMMARY

We have calculated the electronic and structural properties of K_nC_{60} crystals. We found that the enthalpies of reaction for the formation of the alkali-metal–fulleride alloys from C_{60} and metallic K are of the order of 1.4 to 1.7 eV per K atom. The calculated lattice constant is in good agreement with the experimental value and the calculated compressibility for K_3C_{60} is smaller than the compressibility of C_{60}. The valence electron of K is transferred to the C_{60} molecule, and we see a rigid band filling of the lowest unoccupied orbital of C_{60} upon alloying with K. We found that the bandwidth of K_3C_{60} is quite sensitive to pressure.

ACKNOWLEDGMENTS

We thank J. H. Weaver, J. R. Chelikowsky, M. B. Jost, D. M. Poirier, P. J. Benning, C. Gu, T. Ohno, and K. Glassford for stimulating discussions. This research was supported by a computer time grant from the Minnesota Supercomputer Institute. Acknowledgment is made to the Donors of the Petroleum Research Fund, administered by the American Chemical Society, for the partial support of this research.

[1] H. W. Kroto, J. R. Heath, S. C. O'Brian, R. F. Curl, and R. E. Smalley, Nature (London) **318**, 162 (1985).
[2] W. Krätschmer, L. D. Lamb, K. Fostiropoulos, and D. R. Huffman, Nature (London) **347**, 354 (1990).
[3] R. C. Haddon *et al.*, Nature (London) **350**, 320 (1991).
[4] A. F. Hebard *et al.*, Nature (London) **350**, 600 (1991).
[5] R. M. Fleming, A. P. Ramirez, M. J. Rosseinsky, D. W. Murphy, R. C. Haddon, S. M. Zahurak, and A. V. Makhija, Nature (London) **352**, 787 (1991).
[6] N. B. Hannay, T. H. Geballe, B. T. Matthias, K. Andres, P. Schmidt, and D. MacNair, Phys. Rev. Lett. **14**, 225 (1965); I. T. Belash, O. V. Zharikov, and A. V. Palnichenko, Synth. Met. **34**, 455 (1989).
[7] R. M. Fleming, T. Siegrist, P. M. March, B. Hessen, A. R. Kortan, D. W. Murphy, R. C. Haddon, R. Tycko, G. Dabbagh, A. M. Mujsce, M. L Kaplan, and S. M. Zahurak, in *Clusters and Cluster-Assembled Materials*, edited by R. S. Averback, J. Bernholc, and D. L. Nelson, MRS Symposium Proceedings No. 206 (Materials Research Society, Pittsburgh, 1991), p. 691.
[8] P. A. Heiney, J. E. Fischer, A. R. McGhie, W. J. Romanow, A. M. Denenstein, J. P. McCauley, Jr., A. B. Smith III, and D. E. Cox, Phys. Rev. Lett. **66**, 2911 (1991).
[9] S. Liu, Y. Lu, M. M. Kappes, and J. A. Ibers, Science **254**, 408 (1991).
[10] W. I. F. David *et al.*, Nature (London) **353**, 147 (1991).
[11] C. S. Yannoni, R. P. Bernier, D. S. Bethune, G. Meijer, and J. R. Salem, J. Am. Chem. Soc. **113**, 3190 (1991).

[12] K. Herdberg, L. Herdberg, D. S. Bethune, C. A. Brown, H. C. Dorn, R. D. Johnson, and M. de Vries, Science **254**, 410 (1991).
[13] O. Zhou, J. E. Fischer, N. Coustel, S. Kycia, Q. Zhu, A. R. McGhie, W. J. Romanow, J. P. McCauley, Jr., A. B. Smith III, and D. E. Cox, Nature (London) **351**, 462 (1991).
[14] R. M. Fleming, M. J. Rosseinsky, A. P. Ramirez, D. W. Murphy, J. C. Tully, R. C. Haddon, T. Siegrist, R. Tycko, S. H. Glarum, P. Marsh, G. Dabbagh, S. M. Zahurak, A. V. Makhija, and C. Hampton, Nature (London) **352**, 701 (1991).
[15] Q. Zhu, O. Zhu, G. Vaughan, J. P. McCauley, Jr., J. E. Fischer, and A. B. Smith III (unpublished).
[16] P. W. Stephens *et al.*, Nature (London) **351**, 632 (1991).
[17] C. Gu, F. Stepniak, D. M. Poirier, M. B. Jost, P. J. Benning, Y. Chen, T. R. Ohno, J. L. Martins, J. H. Weaver, J. Fure, and R. E. Smalley, Phys. Rev. B **45**, 6348 (1992).
[18] N. Troullier and J. L. Martins, Phys. Rev. B **46**, 1754 (1992).
[19] A general review of the LDA pseudopotential method has been done by W. E. Pickett in Comput. Phys. Rep. **9**, 117 (1989).
[20] J. L. Martins, N. Troullier, and J. H. Weaver, Chem. Phys. Lett. **180**, 457 (1991).
[21] N. Troullier and J. L. Martins, Phys. Rev. B **43**, 1993 (1991).
[22] J. L. Martins and M. L. Cohen, Phys. Rev. B **37**, 6134 (1988).
[23] J. L. Martins, N. Troullier, and S.-H. Wei, Phys. Rev. B **43**, 2213 (1991).
[24] S. G. Louie, S. Froyen, and M. L. Cohen, Phys. Rev. B **26**, 1738 (1982).
[25] L. Kleinman and D. M. Bylander, Phys. Rev. Lett. **48**, 1425 (1982).
[26] X. Gonze, P. Käckell, and M. Scheffler, Phys. Rev. B **41**, 12 264 (1990).
[27] W. Andreoni, F. Gygi, and M. Parrinello (unpublished).
[28] L. Pauling, J. Am. Chem. Soc. **51**, 1010 (1929).
[29] C. Kittel, *Introduction to Solid State Physics*, 6th ed. (Wiley, New York, 1986), p. 76.
[30] S. Saito and A. Oshiyama, Phys. Rev. B **44**, 11 536 (1991).
[31] F. D. Murnaghan, Proc. Natl. Acad. Sci. **30**, 244 (1944).
[32] F. Birch, J. Geophys. Res. **57**, 227 (1952).
[33] P. Vinet, J. Ferrante, J. R. Smith, and J. H. Rose, J. Phys. C **19**, L467 (1986); P. Vinet, J. Ferrante, J. H. Rose, and J. R. Smith, J. Geophys. Res. **92**, 9319 (1987); P. Vinet, J. H. Rose, and J. R. Smith, J. Phys. Condens. Matter **1**, 1941 (1989).
[34] O. Zhou, G. Vaughan, Q. Zhu, J. E. Fischer, P. A. Heiney, N. Coustel, J. P. McCauley, Jr., and A. B. Smith III (unpublished).
[35] J. H. Weaver, J. L. Martins, T. Komeda, Y. Chen, T. R. Ohno, G. H. Kroll, N. Troullier, R. E. Haufler, and R. E. Smalley, Phys. Rev. Lett. **66**, 1741 (1991).
[36] P. J. Benning, D. M. Poirier, N. Troullier, J. L. Martins, J. H. Weaver, R. E. Haufler, L. P. F. Chibante, and R. E. Smalley, Phys. Rev. B **44**, 1962 (1991).
[37] R. C. Haddon, L. E. Brus, and K. Raghavachari, Chem. Phys. Lett. **125**, 459 (1986).
[38] S. C. Erwin and W. E. Pickett, Science **254**, 842 (1991).
[39] W. Y. Ching, M. Huang, Y. Xu, and W. G. Harter, Phys. Rev. Lett. **67**, 2045 (1991); Y. Xu, M. Huang, and W. Y. Ching (unpublished).
[40] P. J. Benning, J. L. Martins, J. H. Weaver, L. P. F. Chibante, and R. E. Smalley, Science **252**, 1417 (1991).
[41] C. T. Chen *et al.*, Nature **352**, 603 (1991).
[42] R. Tycko *et al.*, Science **253**, 884 (1991).
[43] A. Skumanich, Chem. Phys. Lett. **182**, 486 (1991).